Science and Technology Indonesia
e-ISSN:2580-4391 *p*-ISSN:2580-4405
Vol. 9, No. 3, July 2024

Research Paper

Nickel Salt Dependency as Catalyst in the Plating Bath on the Film Properties of Cu/Cu-Ni

Cahaya Rosyidan[1]*, Budhy Kurniawan[2], Bambang Soegijono[3], Mustamina Maulani[1], Lisa Samura[1], Frederik Gresia Nababan[1], Valentinus Galih Vidia Putra[4], Ferry Budhi Susetyo[5]

[1]*Departmen of Petroleum Engineering, Universitas Trisakti, Jakarta, 11440, Indonesia*
[2]*Department of Physics, Universitas Indonesia, Depok, 16424, Indonesia*
[3]*Department of Geoscience, Universitas Indonesia, Depok, 16424, Indonesia*
[4]*Plasma and Nanomaterial Research Group, Politeknik STTT Bandung, Bandung, 40272, Indonesia*
[5]*Department of Mechanical Engineering, Universitas Negeri Jakarta, Jakarta, 13220, Indonesia*
***Corresponding author**: cahayarosyidan@trisakti.ac.id

Abstract
Metal plating frequently employs nickel (Ni) and copper (Cu) as anodes. Cu/ Cu-Ni film formed has many advantages, such as better corrosion resistance and high hardness characteristics. This study aims to assess the properties of Cu/Cu-Ni film, such as phase, surface morphology, crystallographic orientation, hardness, corrosion analysis, and contact angle, which were fabricated using electrodeposition with various Ni salt additions (0.3, 0.5 and 0.7 M). In addition, the cathode current efficiency (CCE) and deposition rate of the Cu/Cu-Ni electrodeposition were also investigated. An increase in Ni salt in the plating bath could enhance the pH, promoting higher CCE and depleting hydrogen evolution at the cathode, leading to the presenting Ni phase in the alloy. The higher concentration of Ni salt in the solution could also enhance the deposition rate due to a shift to a pH value, which affects the roughening of the surface morphology, promoting a higher contact angle. All crystal structures generated by Cu/Cu-Ni electrodeposition were FCC, with the preferred orientation of the (111) plane. Crystallite size and lattice strain depend on the deposition rate. Less crystallite size and lattice strain affect the film's hardness and corrosion resistance. Moreover, the third bath had the resulting Cu-Ni layer with the best hardness and corrosion rate of around 136 HV and 0.081 mmpy.

Keywords
Cathode Current Efficiency, Deposition Rate, Electrodeposition, Corrosion, Hardness

Received: 5 January 2024, Accepted: 4 April 2024
https://doi.org/10.26554/sti.2024.9.3.529-538

1. INTRODUCTION

The electrodeposition procedure is one of the numerous metal coating methods. Metal coating using electrodeposition technology has created many industries that work on coating vehicle engine parts such as pistons, drums, shafts, and other engine parts (Jariwala et al., 2018; Lajevardi et al., 2013). Electrodeposition is done to take advantage of the better properties of the coating element than a substrate. These benefits include heat resistance, a low coefficient of friction, and the prevention of corrosion and erosion properties (Basori et al., 2022; Ghosh et al., 2000; Matsuda et al., 2022). Many factors influence these properties, including solution concentration, temperature, current density, immersion time, pH, and electrical voltage (Kalubowila et al., 2019; Ollivier et al., 2009). Those factors could significantly influence the deposition rate during the electrodeposition process. Moreover, by adjusting the deposition rate, structure, grain size, crystallite size, and surface morphology could be controlled (Augustin et al., 2016; Gomez et al., 2005; Rosyidan et al., 2024).

Metals such as copper (Cu) and nickel (Ni) are commonly employed in metal electrodeposition (Hakim and Pangestu, 2022; Setiamukti et al., 2020). Ni is corrosion resistant and has sufficient strength and hardness properties; meanwhile, Cu is a soft and ductile metal that is not too oxidized by air. Cu's reduction potential (+0.34 V) and Ni's reduction potential (-0.25 V) indicate that copper is nobler than Ni. As a result, Cu ions dissolve in solution via diffusion, and Ni ions dissolve via charge transfer (Ghosh et al., 2006; Goranova et al., 2016). Therefore, the concentration of Ni and Cu needs special attention (Ganesan et al., 2022). In addition, a complexing agent is needed to reduce the potential gap between Ni and Cu. Several studies reported the use of pyrophosphate, citrate, acetate, sulfamate, and glycine as complexing agents (Silaimani et al., 2015).

Ghosh et al. (2000) conducted Ni-Cu plating with PC and DC apparatus using bath composition 0.475 M $NiSO_4.7H_2O$, 0.125 M $CuSO_4.5H_2O$, and 0.2 M sodium citrate (pH was maintained using ammonia solution) and resulting corrosion current between 0.17- 5.77 A cm^{-2} in 3% NaCl, hardness between 384-482 KHN_{50}. Dai et al. (2016) fabricated Ni-Cu film with an electrodeposition technique using 300 g L^{-1} Ni sulfamic acid, 2.5 to 15 g L^{-1} Cu sulfates, 20 g L^{-1} Ni chloride, and 20 g L^{-1} boric acid, resulting in a reduction grain size by increasing Cu content in the alloy. Nady and Negem (2016) studied the electrodeposition of Ni-Cu alloys using various pH and concentration of $NiSO_4$ and $CuSO_4$, with fixed sodium gluconate boric acid and cysteine at 0.025 A cm^{-2} of current density resulting in mostly FCC (111) and FCC (200) crystal planes of the alloys. Goranova et al. (2016) fabricated Ni-Cu using electrodeposition in 0.2 $C_6H_5Na_3O_7.2H_2O$ with different concentrations of Ni salts (0.2, 0.25, 0.5, and 0.6 M $NiSO_4.7H_2O$) and 0.1M $CuSO_4.5H_2O$. The pH (~ 9) was maintained using a 25% NH_4OH solution. The study found that increasing Ni salt (0.6 M $NiSO_4$) has a levelling effect.

Unfortunately, presenting a complexing agent could enhance the cost of production of Cu-Ni alloy. Therefore, presenting a Ni salt as a catalyst (without a complexing agent) in the plating bath needs further investigation. This study aims to create a Cu/Cu-Ni alloy on Cu alloy through electrodeposition and investigate the relationship between physical and hardness-corrosion properties. The layers were made using various solutions at 25°C, and then the CCE and deposition rate were investigated. The Cu/Cu-Ni coating underwent characterization for scanning electron microscope-energy dispersive spectroscopy (SEM-EDS), x-ray diffraction (XRD), hardness, corrosion, and water droplets.

2. EXPERIMENTAL SECTION

2.1 Materials and Preparation

Electrodeposition solutions were made using $CuSO_4.5H_2O$ and $NiSO_4.6H_2O$. All chemicals used in the present research are analytical grade from Merck manufacturer. Pure Cu and Ni were used as an anode, while Cu alloy was used as a cathode with chemical compositions of P 0.22 wt.%, Cd 0.684 wt.%, Si 0.137 wt.%, and Cu balance. Before electrodeposition, the cathode was cleaned using ultrasonic cleaner (DELTA D68H) for 5 min. Electrodeposition was performed with a current density of 30 mA/cm^2 for 1 hour at 25°C using a power supply (SANFIX 305 E). The specimens were electrodeposited using various plating baths, as seen in Table 1.

Table 1. Plating Baths Composition for Cu/Cu-Ni Electrodeposition

Plating Bath	Composition (M)		Measured pH
	$CuSO_4.5H_2O$	$NiSO_4.7H_2O$	
Bath 1	0.1	0.3	2.35
Bath 2	0.1	0.5	2.51
Bath 3	0.1	0.7	2.53

2.2 Characterization

The CCE and deposition rate of the Cu/Cu-Ni electrodeposition were investigated by weighing samples before (initial weight) and after (final weight) electrodeposition and then calculated using equations in the previously reported (Basori et al., 2022; Rosyidan et al., 2024). Afterward, XRD (PANalytical Aeris with Cu K radiation, λ=0.15418 nm, step size=0.02°) was used to determine the crystal structure of the Cu-Ni coating. MAUD software was used to refine and find the crystal parameter using XRD data. Moreover, the Debye-Scherrer formula (Equation 1) was used to calculate the crystal size of various samples (Seakr, 2017).

$$D = \frac{0.9\lambda}{\beta \cos\theta} \quad (1)$$

Where D is the average crystallite size, k is a Scherrer constant of (0.9), λ is radiation wavelength (nm), β is the width of the FWHM diffraction peak (radians), and θ is peak position (° or radians).

FE-SEM equipped with EDS (Thermofisher Quanta 650 EDAX EDS Analyzer) was used to analyze the film surface morphology and phase. Afterward, roughness analysis was performed according to SEM picture using Image J software. Moreover, the hardness of the Cu-Ni film was measured using a MicroMet®5100 Series micro indentation Vickers hardness tester using 100 g of load for 10 s. Measurement was conducted for five spot indentation.

Corrosion investigation was performed using potentiodynamic polarization methods (Digi-Ivy DY2311) in a 3.5% NaCl solution with a volume of 100 ml, the reference electrode being Ag/AgCl and the counter electrode being platinum (Pt) wire. Potentiodynamic polarization was carried out at a speed of 0.002 Vs^{-1} from -1.35 to -0.05 V. Information on corrosion current (i_{corr}) and corrosion voltage (E_{corr}) was acquired from the measurement data using the Tafel extrapolation method. The corrosion rate was calculated using Equation 2 utilizing the corrosion current information (Ahmad, 2006).

$$Cr = C\frac{MI_{corr}}{n_r} \quad (2)$$

Where Cr is the corrosion rate (mmpy), C is a constant for the corrosion rate calculation and is 3.27 mmpy, M is the atomic weight (g mol^{-1}), i_{corr} is corrosion current density (A cm^{-2}), n is the number of electrons involved, and p is the density of Cu and Ni (g cm^{-3}). Last step of the samples characterization is measured water contact angle. The contact angle was observed with a water droplet test on the film surface coated. Some criteria of the angle θ were determined by the value as $\theta < 90°$, $90° \leq \theta < 150°$, and $150° \leq \theta < 180°$ for being

© 2024 The Authors.

hydrophilic, hydrophobic, and super hydrophobic, respectively (Lee et al., 2014).

3. RESULTS AND DISCUSSION

3.1 CCE and Deposition Rate

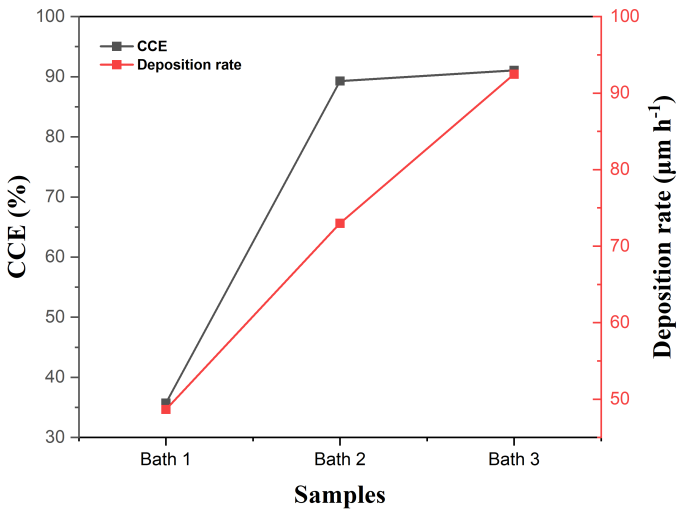

Figure 1. CCE and Deposition Rate for Cu/Cu-Ni Electrodeposited from Bath 1, 2, and 3

Table 2. Average Grain Size Calculation Results of Various Samples

Sample	Grain Size (μm)
Bath 1	105.05
Bath 2	88.22
Bath 3	79.32

Table 3. Average Roughness Value of Various Samples

Sample	Roughness Average (Ra) μm
Bath 1	30.63
Bath 2	37.49
Bath 3	37.82

The composition of $CuSO_4.5H_2O$ and $NiSO_4.6H_2O$ was determined at the start of the experiment. Figure 1 shows the CCE and deposition rate results of various experiments. CCE and deposition rate have similar tendencies; an increase in Ni salt would increase both CCE and deposition rate. CCE refers to the fraction of total current used for metal plating (Rosyidan et al., 2024). At the same time, the deposition rate is the amount of anode material deposited on the cathode at a particular current and time (Park et al., 2008). The first, second, and third solutions had a CCE of 35.71, 89.28, and 91.07%, respectively. The first, second, and third solutions had a deposition rate of 48.66, 72.99, and 92.46, respectively. Hacıismailoğlu and Alper (2011) have found that increased pH leads to increased transient current. Moreover, Rosyidan et al. (2024) have seen that an increase in the current leads to a rise in CCE and deposition rate. Therefore, increased Ni salt promotes increased CCE and deposition rate due to rise and pH (see Table 1).

Table 4. Crystal Parameters of Various Samples

Parameter	Sample Bath 1	Bath 2	Bath 3
Crystal structure		FCC	
Space Group		Fm-3m	
Lattice constant (Å) a = b = c	3.631	3.618	3.612
Cell volume (Å^3)	47.89	47.37	47.14
d-spacing (Å)	1.7530	1.7549	1.7578
Crystallite Size (nm)	43.39	27.54	25.70
Lattice strain	0.27	0.41	0.25

Table 5. Corrosion Measurements of Various Samples

Sample	i_{corr} (A cm^{-2})	E_{corr} (V)	Cr (mmpy)	Criteria
Bath 1	4.40×10^{-6}	-0.261	0.196	Good
Bath 2	5.01×10^{-6}	-0.244	0.223	Good
Bath 3	1.82×10^{-6}	-0.248	0.081	Excellent

Hydrogen evolution could happen at the cathode when electrodeposition is conducted. Hydrogen evolution could disrupt ion's movement to the substrate's surfaces during deposition by blocking the cathode surface. Deo et al. have stated that hydrogen evolution is a competitor at Ni and Cu electrodeposition (Deo et al., 2020). According to the CCE result, higher hydrogen evolution occurred in the samples made using the first solution, and increasing a Ni salt in the solution led to a decrease in hydrogen evolution. Güler et al. (2013) have stated that presenting a hydrogen evolution at the cathode during electrodeposition leads to a decrease in CCE.

3.2 Phase and Surface Morphology

In this study, film deposition involved diffusion and charge transfer by Cu/Cu-Ni. The various films were obtained using a current density of 30 mA cm^{-2} for an hour for all solution variations. The results of the EDS investigation can be seen in Figure 2. Based on Figure 2, it can be seen that 100 wt.% Cu phases are seen when electrodeposited using baths 1 and 2. This means presenting a Ni salt 0.3 and 0.5 M doesn't cause an exhibit of Ni in the film. Meanwhile, when Ni salt concentration rises to 0.7 M, Ni is exhibited in the film around 0.2 wt. %. The solution seems to have a salt limitation, resulting in a Cu-Ni Alloy. Decrease a Cu salt by less than 0.1 M or increasing a Ni salt by more than 0.7 M is needed. Baskaran et al. (2006) electrodeposited Ni using the composition between Ni and Cu salt, which is 20:1.. Sarac et al. (2012) electrodeposited

© 2024 The Authors.

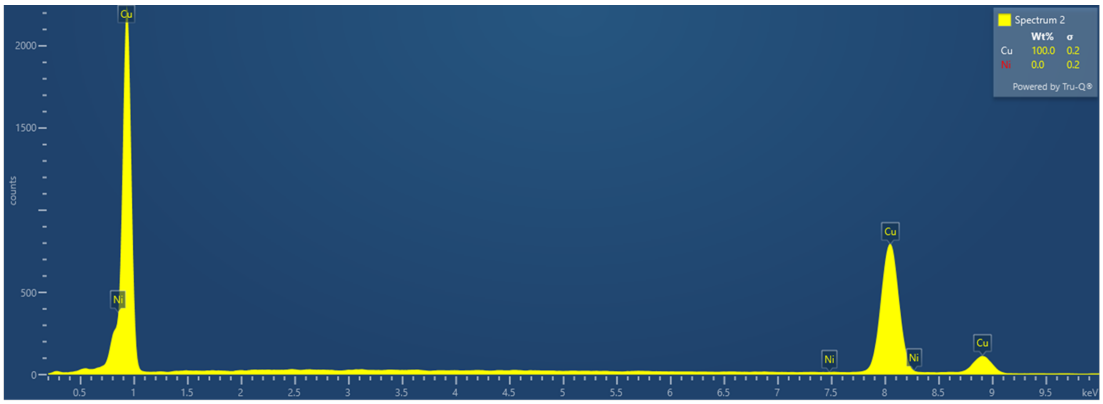

(a)

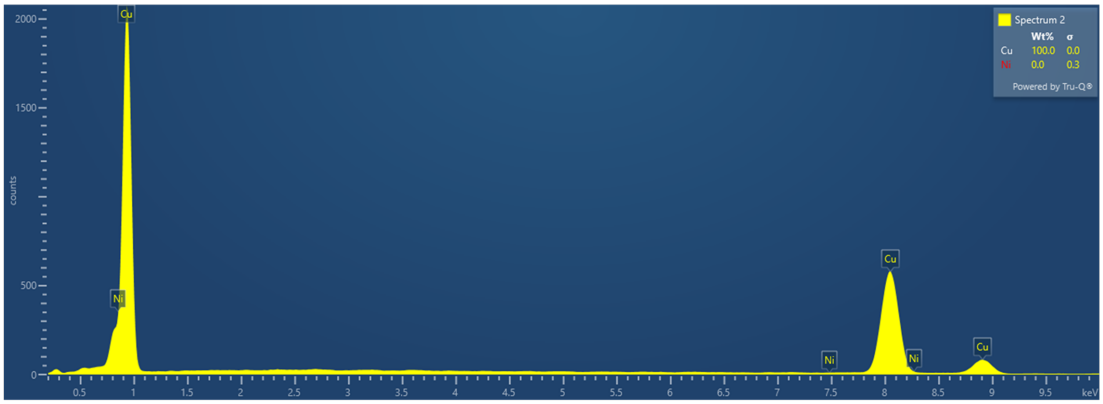

(b)

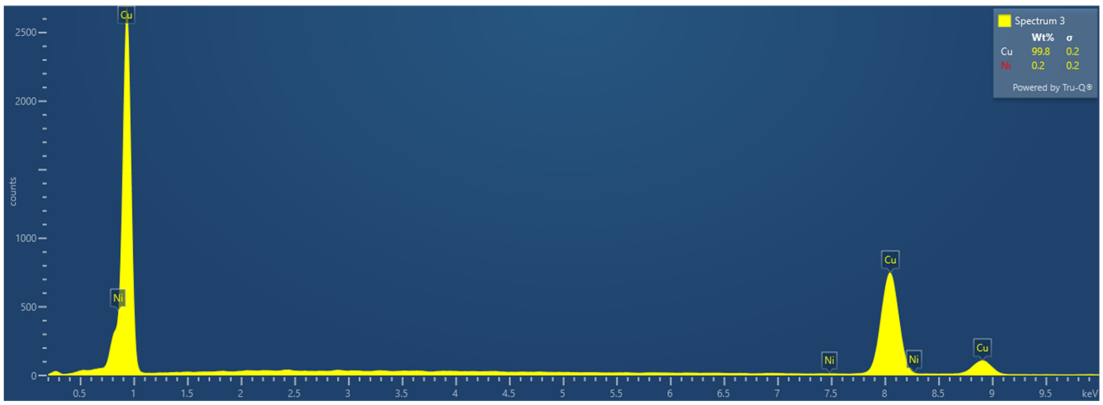

(c)

Figure 2. EDS Test Results of Various Samples

Ni using the composition between Ni and Cu salt are 50:1. Moreover, Hacıismailoğlu and Alper (2011) have stated that hydrogen evolution was occurring at the surface of the substrate during the electrodeposition process, which could prevent the reduction of Ni in the film. This statement is corroborated by the fact that Ni formed in the sample was made using a third solution due to electrodeposition using the first and second solutions, which still caused hydrogen evolution on the substrate surface.

Figures 3 (a)-(c) show the morphology of the deposited non-uniform and compact films, which is affected by the hydrogen evolution. Güler et al. (2013) have stated the disruption is due to hydrogen evolution at the cathode, which could be resulting a non-uniform film. Moreover, pure Cu (Figures 3 (a) and (b)) show morphology with nodules form. In contrast, presenting a Ni in the alloy, which changes nodules to a cauliflower-like

© 2024 The Authors.

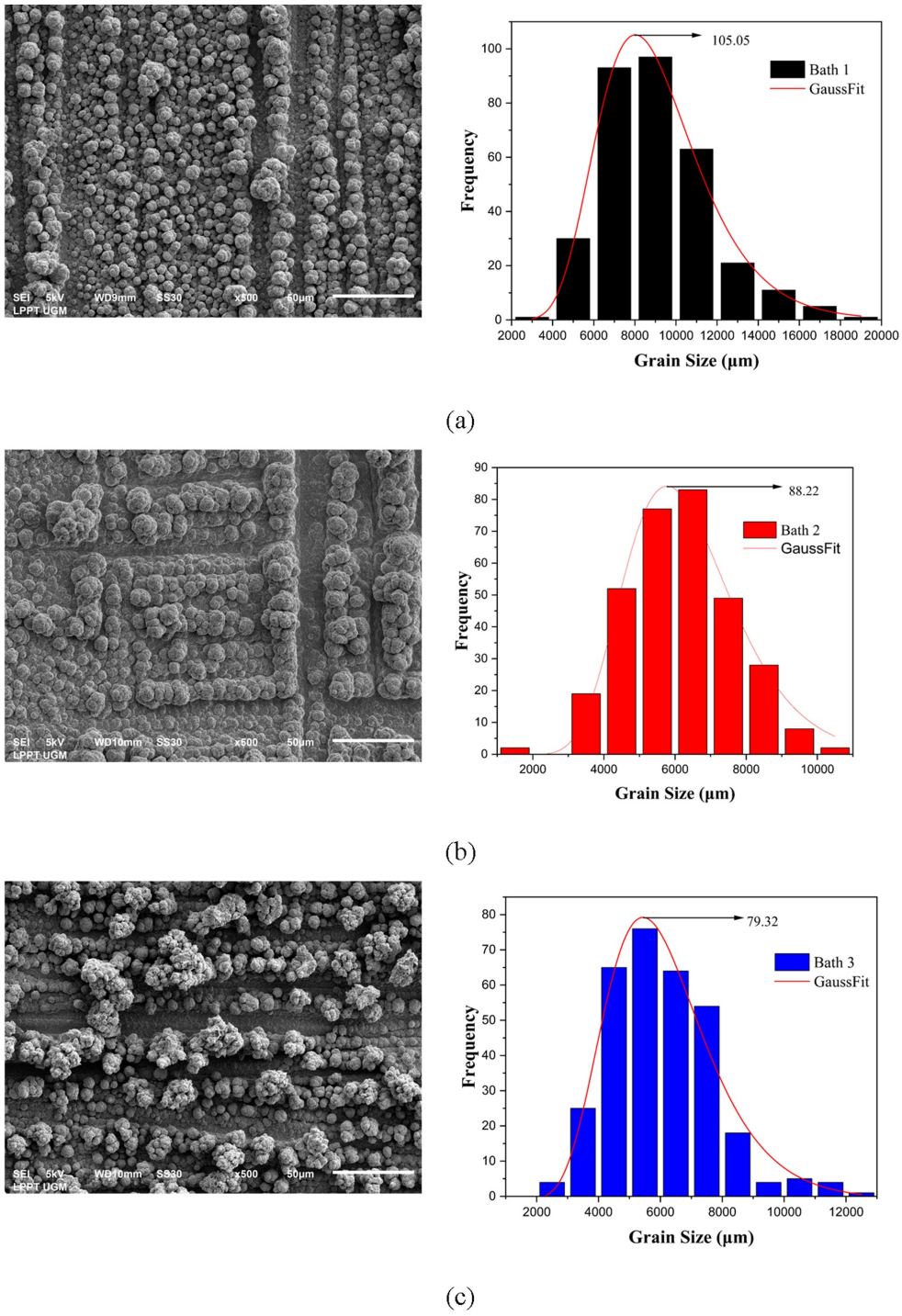

Figure 3. SEM Micrographs and Grain Distribution for Different Samples (a) Bath 1, (b) Bath 2, and (c) Bath 3

form (Figure 3 (c)). As mentioned above, exhibiting a Ni salt in the solution could increase the pH of the solution (Table 1). Kalubowila et al. (2019) have found that increasing the pH bath could transform surface morphology. furthermore, raising a pH solution leads to an increased deposition rate and change in surface morphology. Therefore, there is transformation from nodules to a cauliflower-like form. Statistical analysis using Image J combined Origin with the corresponding Gauss fitting function was used to identify the grain size distribution. The result is presented in Figure 3.

Image J software was used to calculate the average grain size diameter. Table 2 shows the results of calculating the average

© 2024 The Authors.

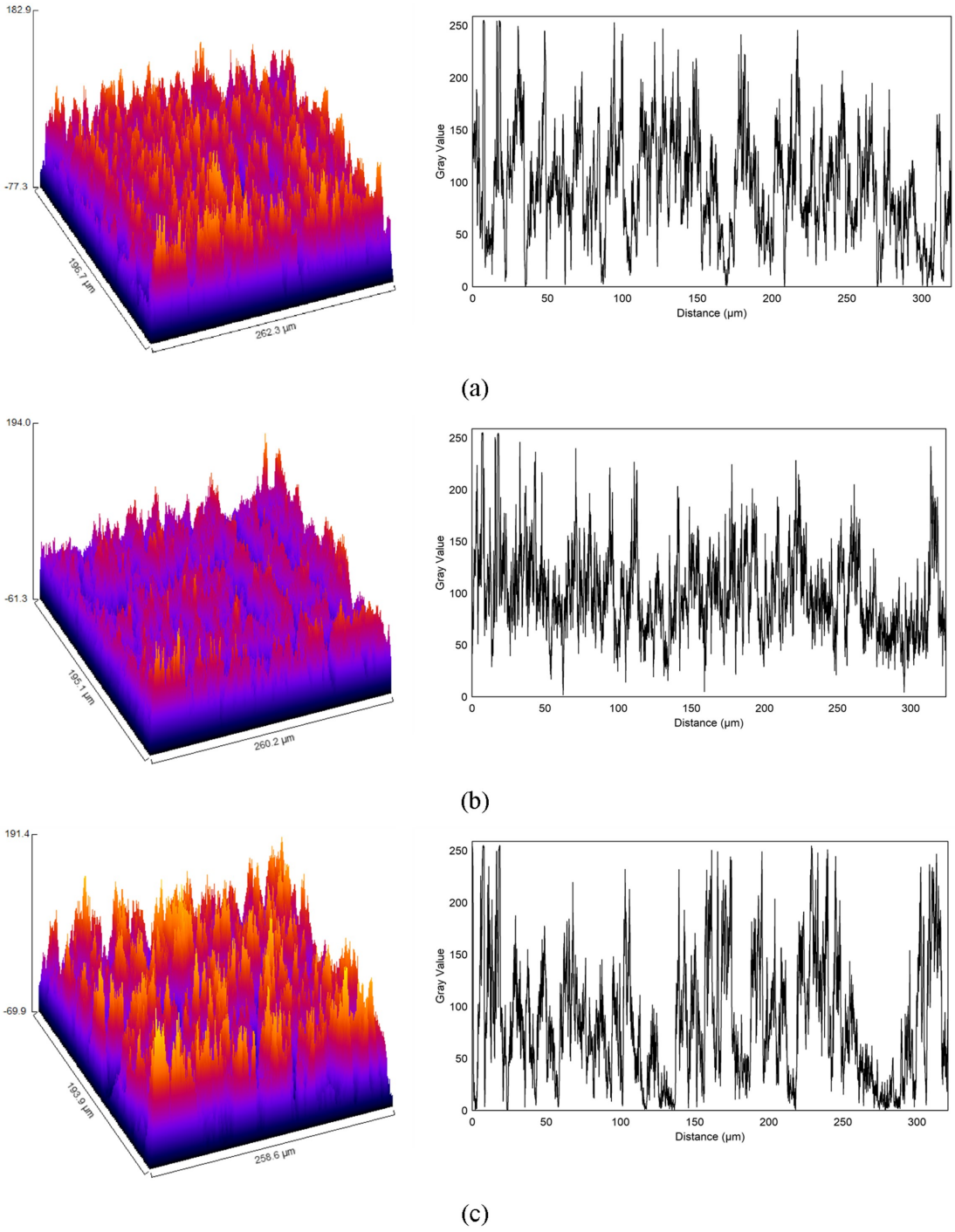

Figure 4. Analysis of Sample sSurfaces Roughness in 3D SEM Image and Graph of Grey Value Against Distance (Left-Right) (a) Bath 1, (b) Bath 2, and (c) Bath 3

grain size. The calculation results show that the grain size average has decreased by increasing the Ni salt in the solution. Baskaran et al. (2006) stated that grain size decreased due to increased electrodeposition current density. Previous research shows that increasing current density increases deposition rate (Rosyidan et al., 2024). Compared to Figure 1, it is seen that rising Ni salt leads to an increased deposition rate. An increase in the deposition rate leads to an increased speed of the ion species deposited on the cathode surface. Therefore, grain size is decreasing in the present research.

Image processing was done using Image J software to obtain detailed information about the resulting image pattern. Image

© 2024 The Authors.

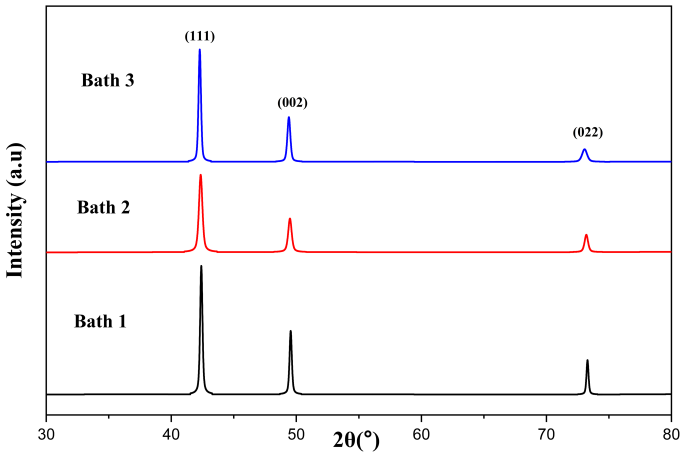

Figure 5. XRD Pattern of Various Samples

patterns were investigated from SEM pictures to interpret the results of surface roughness parameters and 3-D images from surface scanning. The result of the Image J software investigation can be seen in Figure 4, which presents the relationship between distance (μm) and gray value varies with increasing distance.

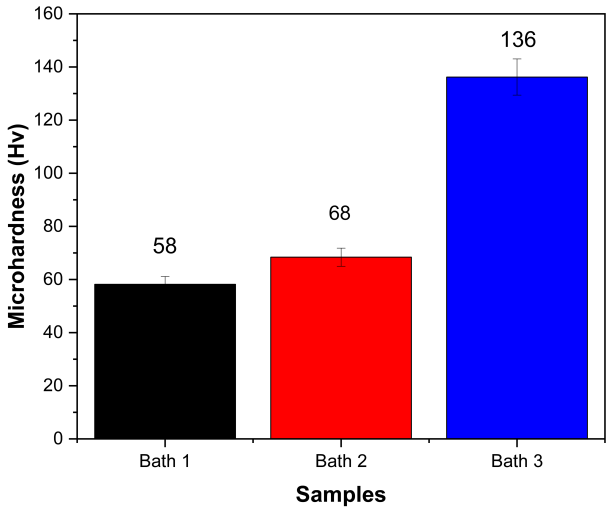

Figure 6. Hardness Test Results of Various Samples

Table 3 shows the average surface roughness of Cu-Ni/Cu coating morphology fabricated from various baths according to Image J software investigation. According to Table 3, increasing Ni salt in the solution increases the films' roughness average. Deo et al. (2020) reported that increasing a current density led to an increase in surface roughness. As mentioned above, increasing current density increases deposition rate (Rosyidan et al., 2024). Compared to the deposition rate measurement (Figure 1), it can be seen that rising Ni salt leads to an increased deposition rate due to pH increments. An increase in the deposition rate leads to an increased speed of the ion species deposited on the cathode surface. Therefore, the roughness average is increased in the present research.

3.3 Crystallographic Orientation

According to the XRD data in Figure 5, three planes formed namely the (111), (002), and (022) planes. The (111) plane dominated when the films were made using baths 1, 2, and 3. The dominance of the (111) plane orientation had benefits such as anticorrosion, increased electrical conductivity, and improved mechanical properties (Seakr, 2017). Moreover, all of the collected XRD data were then analyzed using MAUD software, and the crystal parameters are shown in Table 4. All led to the same crystal structure and space group, FCC and Fm-3m, which can be concluded that atoms of the Cu and Ni form a substitutional solid solution (Dai et al., 2016).

Table 4 shows that the lattice constant and cell volume decrease due to the increase in the Ni phase in the alloy, which perfectly agrees with other reports (Baskaran et al., 2006). Moreover, increased Ni salt in the plating bath decreases crystallite size. Augustin et al. (2016) have reported an increase in current density promoting reduced crystallite size. Increasing the electrodeposition process's current density influences the deposition rate's increase; the amount of ion species deposited on the cathode rose; therefore, crystallite size decreased. Small crystal size indicates that the distance between grains is close, contributing to material qualities with more roughness properties (Dai et al., 2016). This result is in perfect agreement with the average roughness in Table 3. Moreover, a smaller lattice strain is seen in the sample made using bath 3.

3.4 Hardness

Hardness is a material's resistance to plastic deformation. A coating procedure is considered successful if it can enhance the qualities of the coated objects. One of the purposes of electrodeposition in the present research is to improve material deposited hardness. The results of the hardness of the coating were obtained using a Vickers micro-hardness tester. The Vickers microhardness method obtained 58 HV in the first solution, 68 HV in the second solution, and 136 HV in the third solution. It seems an increase in Ni salt would increase the hardness. In their study, Augustin et al. found that a decrease in crystallite size promotes an increase in hardness, which is in perfect agreement with the present research (Augustin et al., 2016). Besides crystallite size, the exhibit of Ni in the alloy also influences the hardness of the sample (Rosyidan et al., 2024). As seen in Figure 6, a sample was made using bath 3, resulting in higher hardness, which is affected by the exhibit of Ni in the alloy. According to the EDS result, only one sample was made using bath 3, resulting in Ni in the alloy. Compared to the Monel 400, hardness is between 150 to 200 HV, and present research has lower hardness (Kukliński et al., 2020).

3.5 Corrosion

Figure 7 shows the corrosion curves of the electrodeposition of Cu/Cu-Ni on the Cu alloy substrate. The i_{corr} and E_{corr}

© 2024 The Authors.

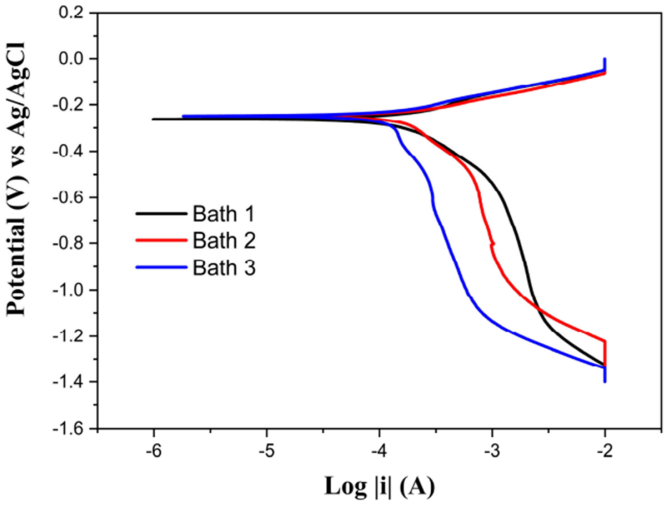

Figure 7. Corrosion Curve for Various Samples

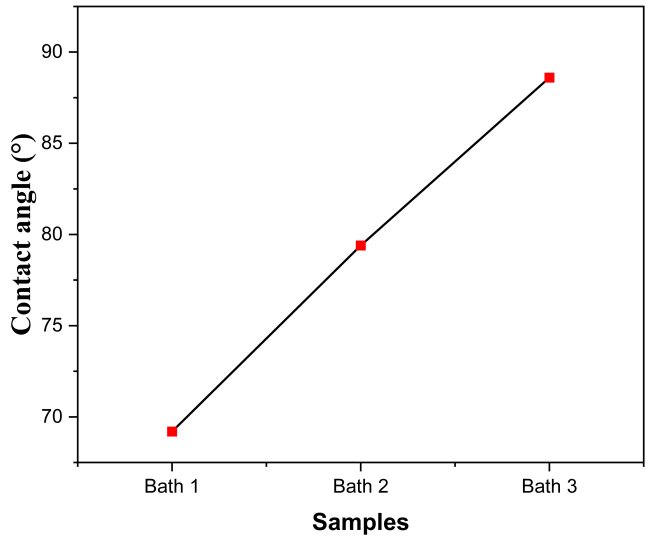

Figure 8. Water contact angle of various samples

were found using the Tafel extrapolation method. Meanwhile, CR was calculated using Equation (2). The summary of the calculations for the CR of various samples is shown in Table 5. The crystal plane could determine the corrosion rate behavior of materials with the FCC crystal system. The (111) crystal plane is more corrosion-resistant in materials with the FCC system than the (002) and (022) crystal planes (Al Kharafi et al., 2012). Therefore, all of the samples met good and excellent criteria. Moreover, based on Table 5, it can be seen that the third solution has the best corrosion rate. This behavior is influenced by the lattice strain that was formed. Lattice strain is sample defect concentration measured due to a void core in the lattice (Basori et al., 2023). Therefore, the smallest lattice strain leads to the highest corrosion resistance. According to Wang et al. and Ghosh et al. studies, Monel-400 i_{corr} is 2.24 $\times 10^{-6}$ and 2.2 $\times 10^{-6}$ (A cm^{-2}) (Ghosh et al., 2000; Wang et al., 2014). Compared with Table 5, it can be seen that the sample made using a third solution has lower i_{corr} than Monel-400.

3.6 Contact Angle

The water droplet test can be used to determine the hydrophilic, hydrophobic, and superhydrophobic properties of a film. Figure 8 shows a snapshot of the drip test findings for various samples. All samples possess hydrophilic properties since they have contact angles between 0° and 90° (Thurber et al., 2016). The contact angles achieved in the first, second, and third solution 1 are 69.2°, 79.4° and 88.6°, respectively. Increnement of the water contact angle is probably due to an increased film surface roughness. In their research, Huang et al. found that increasing roughness would increase the water contact angle (Huang and Gates, 2020). Moreover, Yu et al. found that increasing electrolyte pH from 2 to 4 increases the film's water contact angle (Yu et al., 2013), probably due to an increase in the surface roughness of the samples.

4. CONCLUSIONS

Cu/Cu-Ni film was electrodeposited onto Cu alloy using various bath compositions, and according to the multiple findings, increased Ni salt content led to increased deposition rate and CCE due to an increased pH and depleting hydrogen evolution, which impacted grain size, more roughness, less crystallite size and presenting small amount of a Ni in the film. The formed crystal structure was a single-phase FCC with the dominant (111) plane. The hardness increment is due to a decrease in crystallite size. Lesser lattice strain contributed to a higher corrosion resistance. The films have more roughness and impact on the higher water contact angle. The 99.8Cu0.3Ni alloy has the best corrosion resistance and is recommended as an alternative to change Monel-400.

5. ACKNOWLEDGMENT

This project was financially supported by Universitas Trisakti based on the assignment letter number 800/C-4/FTKE/USA KTI/X/2023.

REFERENCES

Ahmad, Z. (2006). *Principles of Corrosion Engineering and Corrosion Control*. 1th edition. Elsevier

Al Kharafi, F., I. Ghayad, and R. Abdullah (2012). Corrosion Inhibition of Copper in Non-Polluted and Polluted Sea Water Using 5-Phenyl-1-H-Tetrazole. *International Journal of Electrochemical Science*, **7**(4); 3289–3298

Augustin, A., P. Huilgol, K. R. Udupa, and U. Bhat (2016). Effect of Current Density during Electrodeposition on Microstructure and Hardness of Textured Cu Coating in the Application of Antimicrobial Al Touch Surface. *Journal of the mechanical behavior of Biomedical materials*, **63**(October); 352–360

© 2024 The Authors.

Baskaran, I., T. S. Narayanan, and A. Stephen (2006). Pulsed Electrodeposition of Nanocrystalline Cu–Ni Alloy Films and Evaluation of Their Characteristic Properties. *Materials Letters*, **60**(16); 1990–1995

Basori, B. Soegijono, and F. Susetyo (2022). Magnetic Field Exposure on Electroplating Process of Ferromagnetic Nickel Ion on Copper Substrate. In *Journal of Physics: Conference Series*, volume 2377. IOP Publishing, page 012002

Basori, B., B. Soegijono, S. Yudanto, D. Nanto, and F. Susetyo (2023). Effect of Low Magnetic Field during Nickel Electroplating on Morphology, Structure, and Hardness. In *Journal of Physics: Conference Series*, volume 2596. IOP Publishing, page 012014

Dai, P., C. Zhang, J. Wen, H. Rao, and Q. Wang (2016). Tensile Properties of Electrodeposited Nanocrystalline Ni-Cu Alloys. *Journal of Materials Engineering and Performance*, **25**(January); 594–600

Deo, Y., S. Guha, K. Sarkar, P. Mohanta, D. Pradhan, and A. Mondal (2020). Electrodeposited Ni-Cu Alloy Coatings on Mild Steel for Enhanced Corrosion Properties. *Applied Surface Science*, **515**(June); 146078

Ganesan, M., C.-C. Liu, S. Pandiyarajan, C.-T. Lee, and H.-C. Chuang (2022). Post-Supercritical CO_2 Electrodeposition Approach for Ni-Cu Alloy Fabrication: An Innovative Eco-Friendly Strategy for High-Performance Corrosion Resistance with Durability. *Applied Surface Science*, **577**(1); 151955

Ghosh, S., A. Grover, G. Dey, U. Kulkarni, R. Dusane, A. Suri, and S. Banerjee (2006). Structural Characterization of Electrodeposited Nanophase Ni–Cu Alloys. *Journal of Materials Research*, **21**(1); 45–61

Ghosh, S., A. Grover, G. Dey, and M. Totlani (2000). Nanocrystalline Ni–Cu Alloy Plating by Pulse Electrolysis. *Surface and Coatings Technology*, **126**(1); 48–63

Gomez, E., S. Pane, and E. Valles (2005). Electrodeposition of Co–Ni and Co–Ni–Cu Systems in Sulphate–Citrate Medium. *Electrochimica Acta*, **51**(1); 146–153

Goranova, D., R. Rashkov, G. Avdeev, and V. Tonchev (2016). Electrodeposition of Ni–Cu Alloys at High Current Densities: Details of the Elements Distribution. *Journal of Materials Science*, **51**(June); 8663–8673

Güler, E. S., E. Konca, and İ. Karakaya (2013). Effect of Electrodeposition Parameters on the Current Density of Hydrogen Evolution Reaction in Ni and Ni-MoS_2 Composite Coatings. *International Journal of Electrochemical Science*, **8**(4); 5496–5505

Hacıismailoğlu, M. Ş. and M. Alper (2011). Effect of Electrolyte pH and Cu Concentration on Microstructure of Electrodeposited Ni-Cu Alloy Films. *Surface and Coatings Technology*, **206**(6); 1430–1438

Hakim, M. S. and H. Pangestu (2022). Preparation and Application of Nickel Electroplating on Copper (Ni/EC) Electrode for Glucose Detection. *Science and Technology Indonesia*, **7**(2); 208–212

Huang, X. and I. Gates (2020). Apparent Contact Angle around the Periphery of a Liquid Drop on Roughened Surfaces. *Scientific Reports*, **10**(1); 8220

Jariwala, F., R. Gohil, P. Trivedi, J. Parmar, B. Borda, S. Patel, B. Goyal, and V. Rao (2018). Electroplating of Nickel and Chromium on Aluminum 6082-T6 Alloy. Proceedings of the International Conference on Recent Advances in Metallurgy for Sustainable Development, pages 1–3

Kalubowila, K., K. Jayathileka, L. Kumara, K. Ohara, S. Kohara, O. Sakata, M. Gunewardene, J. Jayasundara, D. Dissanayake, and J. Jayanetti (2019). Effect of Bath pH on Electronic and Morphological Properties of Electrodeposited Cu_2O Thin Films. *Journal of The Electrochemical Society*, **166**(4); D113

Kukliński, M., A. Bartkowska, D. Przestacki, and G. Kinal (2020). Influence of Microstructure and Chemical Composition on Microhardness and Wear Properties of Laser Borided Monel 400. *Materials*, **13**(24); 5757

Lajevardi, S., T. Shahrabi, J. Szpunar, A. S. Rouhaghdam, and S. Sanjabi (2013). Characterization of the Microstructure and Texture of Functionally Graded Nickel-Al_2O_3 Nano Composite Coating Produced by Pulse Deposition. *Surface and Coatings Technology*, **232**(October); 851–859

Lee, J. M., K. M. Bae, K. K. Jung, J. H. Jeong, and J. S. Ko (2014). Creation of Microstructured Surfaces Using Cu–Ni Composite Electrodeposition and Their Application to Superhydrophobic Surfaces. *Applied Surface Science*, **289**(January); 14–20

Matsuda, T., R. Saeki, M. Hayashida, and T. Ohgai (2022). Microhardness and Heat-Resistance Performance of Ferromagnetic Cobalt-Molybdenum Nanocrystals Electrodeposited from an Aqueous Solution Containing Citric Acid. *Materials Research Express*, **9**(4); 046502

Nady, H. and M. Negem (2016). Ni-Cu Nano-Crystalline Alloys for Efficient Electrochemical Hydrogen Production in Acid Water. *RSC Advances*, **6**(56); 51111–51119

Ollivier, A., L. Muhr, S. Delbos, P. Grand, M. Matlosz, and E. Chassaing (2009). Copper–Nickel Codeposition As a Model for Mass-Transfer Characterization in Copper–Indium–Selenium Thin-Film Production. *Journal of Applied Electrochemistry*, **39**(May); 2337–2344

Park, B. N., Y. S. Sohn, and S. Y. Choi (2008). Effects of a Magnetic Field on the Copper Metallization Using the Electroplating Process. *Microelectronic Engineering*, **85**(2); 308–314

Rosyidan, C., B. Kurniawan, B. Soegijono, V. Vidia Putra, D. R. Munazat, and F. B. Susetyo (2024). Effect of Current Density on Magnetic and Hardness Properties of Ni-Cu Alloy Coated on Al Via Electrodeposition. *International Journal of Engineering*, **37**(2); 213–223

Sarac, U., R. M. Öksüzoğlu, and M. C. Baykul (2012). Deposition Potential Dependence of Composition, Microstructure, and Surface Morphology of Electrodeposited Ni–Cu Alloy Films. *Journal of Materials Science: Materials in Electronics*, **23**(April); 2110–2116

Seakr, R. (2017). Microstructure and Crystallographic Characteristics of Nanocrystalline Copper Prepared from Acetate

© 2024 The Authors.

Solutions by Electrodeposition Technique. *Transactions of Nonferrous Metals Society of China*, **27**(6); 1423–1430

Setiamukti, D., A. Khusnani, and M. Toifur (2020). The Effect of Electrolyte Concentration on the Sensitivity of Low-Temperature Sensor Performance of Cu/ni Film. *Science and Technology Indonesia*, **5**(2); 28–33

Silaimani, S., G. Vivekanandan, and P. Veeramani (2015). Nano-Nickel-Copper Alloy Deposit for Improved Corrosion Resistance in Marine Environment. *International Journal of Environmental Science and Technology*, **12**(May); 2299–2306

Thurber, C. R., Y. H. Ahmad, S. F. Sanders, A. Al-Shenawa, N. D'Souza, A. M. Mohamed, and T. D. Golden (2016). Electrodeposition of 70-30 Cu-Ni Nanocomposite Coatings for Enhanced Mechanical and Corrosion Properties. *Current Applied Physics*, **16**(3); 387–396

Wang, S., X. Guo, H. Yang, J. Dai, R. Zhu, J. Gong, L. Peng, and W. Ding (2014). Electrodeposition Mechanism and Characterization of Ni-Cu Alloy Coatings from a Eutectic-Based Ionic Liquid. *Applied Surface Science*, **288**(January); 530–536

Yu, Q., Z. Zeng, W. Zhao, M. Li, X. Wu, and Q. Xue (2013). Fabrication of Adhesive Superhydrophobic Ni-Cu-P Alloy Coatings with High Mechanical Strength by One Step Electrodeposition. *Colloids and Surfaces A: Physicochemical and Engineering Aspects*, **427**(June); 1–6

© 2024 The Authors.